Experimental Comparison of Two-Phase Heat Spreaders for Space Modular Electronics

Sai Kiran Hota[1], Kuan-Lin Lee[2], Greg Hoeschele[3], Tanner Mcfarland[4], Srujan Rokkam[5], Richard W. Bonner[6]
Advanced Cooling Technologies, Inc, Lancaster, PA, 17601

Standardized form factor electronics cards promote inter-operability across various applications on land and in space. However, current cards might be less reliable due to thermal management bottlenecks. Conventional approaches for cooling electronics cards involve using conduction based thermal heat spreaders, which are limited in performance. So, to improve thermal management of these electronics, high thermal performing, two-phase based heat spreaders are gaining attention. Among these two-phase heat spreaders, embedded heat pipe has achieved high maturity, while, pulsating heat pipes (PHPs) are in nascent stages. In an ongoing SBIR Phase II program funded by NASA, Advanced Cooling Technologies, Inc. is developing a PHP heat spreader for standard 3U form factor electronics thermal management. A prototype PHP was fabricated by 3D printing approach with aluminum as the base plate. Performance of the PHP was determined and compared to a HiK™ plate, which is a copper-water embedded heat pipe heat spreader of same form factor. The experiments were performed on an assembled platform with one central evaporator and two edge condenser configurations. The evaporator was a 1-inch x 1-inch aluminum block with two cartridge heater inserts. A copper tube pressed aluminum cold plate was used as the condenser. Influence of operating parameters such as operating temperature and orientation were determined.

Nomenclature

C	=	Thermal conductance, W/°C
C_p	=	Specific heat capacity, J/kg-K
d	=	Diameter, m
h_{fg}	=	Enthalpy of Vaporization, J/kg
M_{php}	=	PHP merit number
Q	=	Heat load, W
R	=	Gas constant, J/kg-K
ΔT	=	Temperature difference, °C
Z	=	Compressibility factor

Greek letters

μ	=	Dynamic viscosity, Pa.s
ρ	=	Density, kg/m³
σ	=	Surface tension, N/m

Abbreviations

EHP	=	Embedded Heat Pipe (HiK™ plate)
HTF	=	Heat Transfer Fluid
PHP	=	Pulsating Heat Pipe
SBIR	=	Small Business Innovation Research

---

[1] R&D Engineer II, Advanced Cooling Technologies, Inc., 1046 New Holland Ave., Lancaster, PA 17601
[2] Lead Engineer-R&D, Advanced Cooling Technologies, Inc., 1046 New Holland Ave., Lancaster, PA 17601
[3] Lead Engineer- PD, Advanced Cooling Technologies, Inc., 1046 New Holland Ave., Lancaster, PA 17601
[4] PD Engineer, Advanced Cooling Technologies, Inc., 1046 New Holland Ave., Lancaster, PA 17601
[5] Group Manager-R&D, Advanced Cooling Technologies, Inc., 1046 New Holland Ave., Lancaster, PA 17601
[6] Vice President, R&D, Advanced Cooling Technologies, Inc., 1046 New Holland Ave., Lancaster, PA 17601

I. Introduction

Standardizing power electronics architecture is of relevance to promote interoperability, minimize overall costs associated with developing unique parts, and to reduce engineering and logistics costs [1]. This will greatly improve the interoperability of the electronics cards across various space missions which is of relevance to NASA and other space agencies. Space electronics architectures typically follow the SpaceVPX™ standards recommended by the VITA 78 and VITA 78.1 working groups [2]. The spaceVPX standards are used by NASA, JPL, L3 Communications, Northrop Gruman, ESA, etc. The hardware standards are derived from general open architectural electronics specifications which for cards cooling is based on VITA 48.2 standards [2].

Rapid technological advances in semiconductors spurred transition to smaller transistors ensued significant increase in heat flux dissipation. This waste heat must be dissipated to keep the electronics within safe operating temperatures, typically < 75 °C [3], for reliable operations. This poses a thermal management challenge, especially in light of interest in standardizing electronics cards and module architectures. Thermal heat spreaders are employed to dissipate waste heat flux from these electronics. However, conventional heat spreaders are conduction based with limited thermal conductivity, which may not be sufficient to meet temperature requirements at high heat loads. To tackle this challenge, two-phase heat transfer-based heat spreaders such as heat pipes or vapor chamber have been developed with notable success. In two-phase heat spreaders, the heat transfer is by a saturated two-phase working fluid. Heat pipes embedded in the base plate, or internal channel Pulsating Heat Pipe (PHP) plate are two of such two-phase plate heat spreaders being actively investigated in electronics cooling.

Embedded heat pipe (EHP) heat spreaders are gaining significant commercial success, e.g., HiK™ plate [4]. In an EHP, the heat from the electronics vaporizes the working fluid in the evaporator section. The vapor then flows to the condenser where it condenses and returns to the evaporator. The equivalent thermal conductivity of the plate is typically between 600-1200 W/m-K, and can nominally handle a heat load up to 70 W/cm^2 [5] depending on the geometry and operating conditions. In a PHP, the working fluid distributes naturally into liquid slug and vapor plug in the capillary fluid channels. The heat from the electronics chips partially vaporizes the liquid slug of the working fluid, thereby increasing the vapor pressure. Simultaneously, the vapor plug in the condenser shrinks or collapses decreasing the pressure. This interplay of pressure differential instigates pulsations in the working fluid [6]. The heat transfer limit of the PHP depends on a number of factors like the geometry, operating condition, working fluid, etc. but can be up to 50 W/cm^2 or higher [7,8].

These two-phase heat spreader technologies have typically been independently studied and the performance has usually been compared to the baseline case of conduction heat spreader. It is of scientific relevance to determine the more appropriate heat spreader technology for a given operational condition. In the past, the authors have demonstrated up to 100% improvement in heat transfer performance with both HiK™ plate heat spreader-based electronics cooling system and PHP based electronics cooling system [8]. Experimental heat transfer comparison between the two-heat spreaders for a flat plate 6U standard form factor (233 mm x 160 mm) [9] showed that propylene PHP had better performance over EHP at lower operating temperatures, while, the EHP performed better than the PHP at temperatures above 20 °C [10]. In this manuscript, a comparative performance study of the two-phase heat spreaders for a standard 3U form factor (100 mm x 160 mm) [9] electronics heat spreader is described, and the performance characteristics are noted.

The organization of the manuscript is as follows: In section II, mechanical specifications of the heat spreaders- the EHP and the PHP are described, trade study of the heat transfer limits is described; In section III, experimental methodology and test parameters are explained; In section IV, comparative experimental performance of the heat spreaders is reported; In section V, near term future plans are described; and in section VI, the conclusions and key takeaways presented in the manuscript are noted.

II. Geometric Specification and Trade Study of the Heat Spreaders

The heat spreaders were fabricated for 3U form factor electronics according to VITA 48.2 standards for electronics cards. The geometric specifications of the heat spreader are shown in Figure 1. The heat spreader is 6.3-inches long (160 mm) and 3.937-inches (100 mm) wide. The thickness of the heat spreader is 0.133-inches (3.38 mm). The heat spreader has a step plane for integrating with the electronics enclosure via a card retainer. In this manuscript, Isothermal Card Edge (ICE-Lok®) [11] was used as the electronics card retainer. The width of the step plane is 0.365-inches (9.27 mm), resulting in the electronics (heat source) plane width of 2.941-inches (74.7 mm). The height of the stepped plane for the card retainer integration is 0.527-inches (13.38 mm). Holes were provided along the stepped plane to mechanically fasten the heat spreader to the card retainer.

The design and trade study of the EHP and the PHP explained below considers a central 1-inch x 1-inch heater and two (stepped) edge heat rejection configurations.
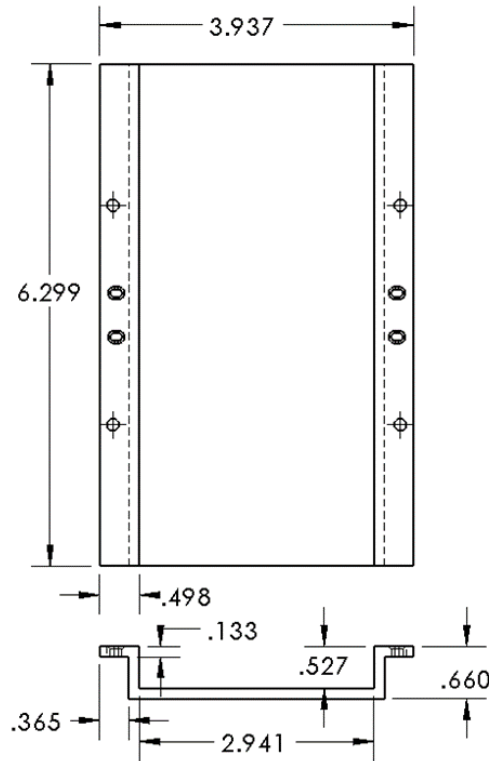
Figure 1. Geometric specification of 3U form factor heat spreader (dimensions in inches)

A. Design and trade study of EHP (HiK™) plate heat spreader

An EHP heat spreader was designed based on the above-mentioned specifications and analyzed prior to fabrication for performance testing. The EHP is essentially copper-water heat pipes embedded into an aluminum baseplate. The heat pipes incorporate copper mesh wick structures for capillary transport of the working fluid back to the evaporator. The design and analysis of the heat spreaders are explained here under.
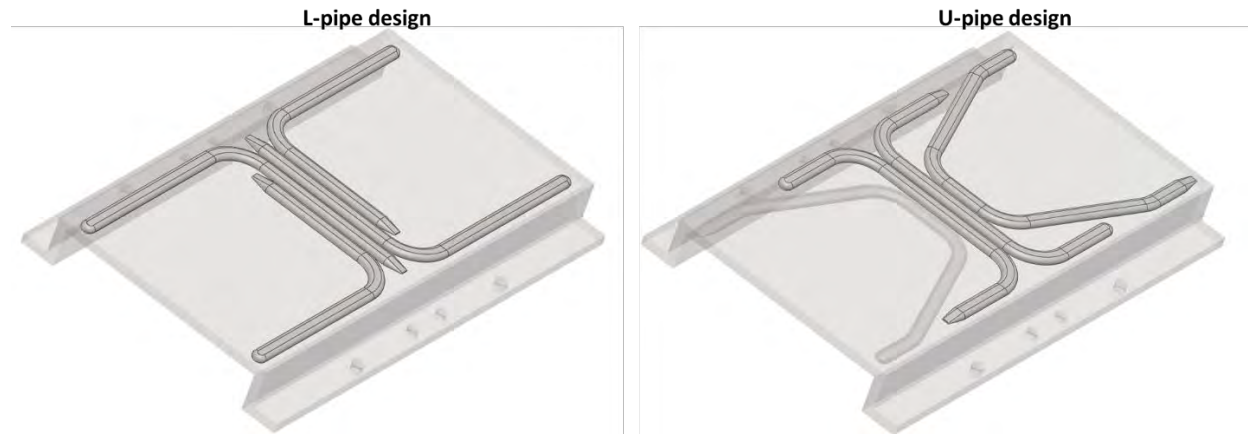
Figure 2. L-pipe and U-pipe designs of EHP heat spreader

Two heat pipes designs: L-shape layout, and U-shape layout were selected as shown in Figure 2. The EHP has 4 copper-water heat pipes symmetrical along the central plane of the baseplate. The heat pipes were packed tightly near the center under the heat source location. The condenser portion of the heat pipes is near the stepped edge but on the same plane as the heat source. The heat transfer along the stepped edge to the card retainer for heat rejection is thereby

3

limited by material conduction. The distinction between the heat pipes in the L-shape layout and U-shape layout is summarized in Table 1.

Table 1. Distinction between L-pipe design and U-pipe design of the EHP

Parameter	L-pipe design	U-pipe design
No of screen wraps	2	
Screen material/ type	Cu/ 150	
Heat pipe diameter	4 mm	
Flattened height	2.67 mm	
Flattened width	4.88 mm	
Total length of heat pipe (range)	118.1 mm – 134.6 mm	140.6 mm – 172.1 mm
Length of heat pipe in evaporator	25.4 mm	12.7 mm
Length of heat pipe in condenser (range)	53.3 mm – 59.7 mm	21.6 mm – 26.7 mm
No of effective heat pipes	4	8
Evaporator length	25.4 mm	12.7 mm
Condenser length	58.4 mm	17.8 mm
Weight of the EHP	187.55 g	188.35 g
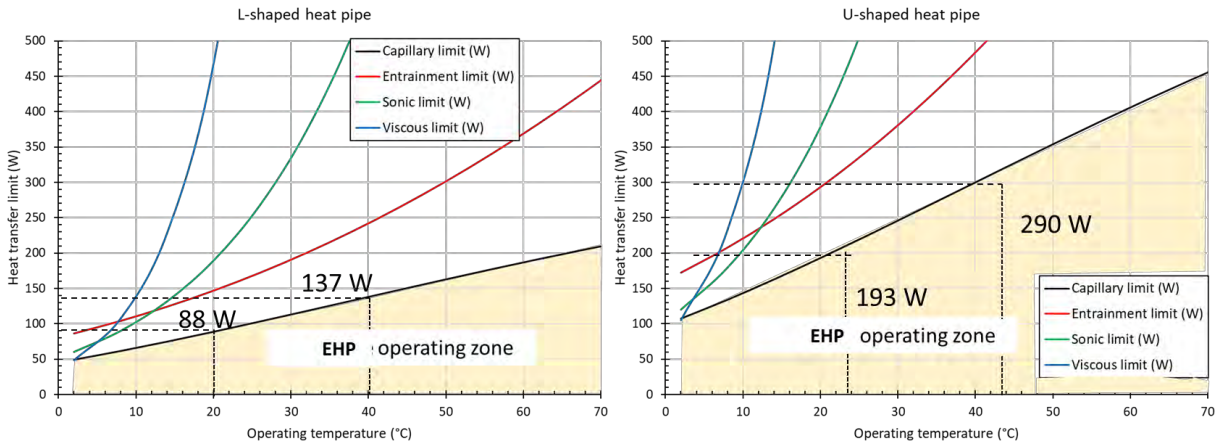
Figure 3. Anticipated heat transfer limits of the EHP heat spreaders for the L-pipe and U-pipe designs

Trade study was then performed on the two EHP heat spreader designs. Figure 3 shows the heat transfer limits of the L-pipe and U-pipe design of the EHP heat spreader. The maximum heat transfer of the EHP is constrained by the capillary limit. At an operating temperature of 20 °C, the maximum heat transfer limit with the L-pipe design was predicted to be 88 W, which increases to 137 W at 40 °C. The U-pipe design, on the other hand, had at least two times more heat transfer capability compared to the L-pipe design. At an operating temperature of 20 °C, the maximum heat transfer limit of the U-pipe design was 193 W, which was 120% more than the L-pipe design. Likewise, at an operating temperature of 40 °C, the heat transfer limit of the U-pipe design was 290 W, which was 112% more than the L-pipe design.

B. Design and trade study of PHP heat spreader

A PHP heat spreader with design, shown in Figure 4. The PHP channel layout is adapted from previous PHP demonstration [8] and representative of the chosen central heating and edge heat rejection configuration. The PHP channel layout was symmetrical along the central plane. The PHP channel diameter was 1/16-inches (~ 1.6 mm). Total number of PHP channel turns under the heat source was 8 and the total number of PHP channel turns under the card retainer (heat rejection) was 48. The total PHP evaporator length was 7.75 -inches (196.8 mm) and the total condenser length was 20.3-inches (515.5 mm).

Based on the chosen working operating temperature ranges, working fluid selection was first performed by determining the maximum (critical) PHP channel diameter based on the Bond number limit, which is given as:

$$d_{crit} = 2\sqrt{\frac{\sigma}{g(\rho_l - \rho_v)}}$$

eq. 1

4

Where, σ is the surface tension, ρ_l is the liquid density, and ρ_v is the vapor density.
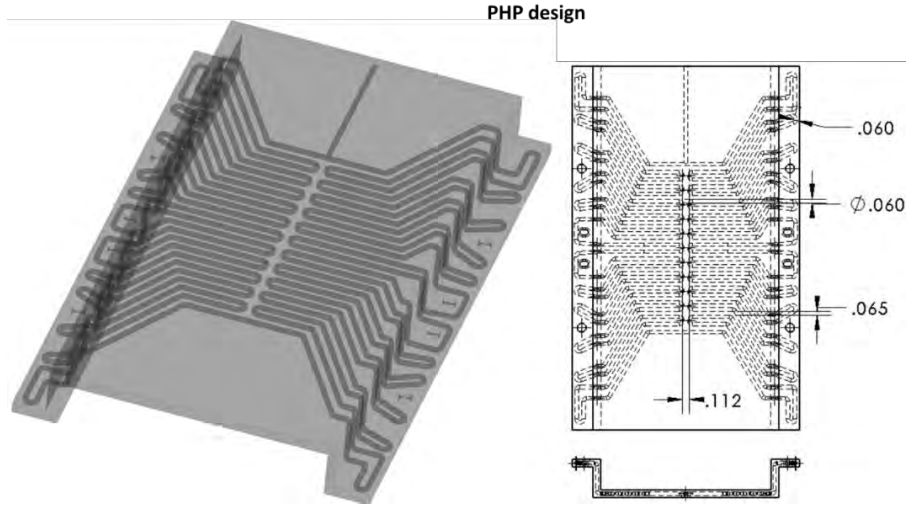

Figure 4. PHP channel layout and geometrical specifications of the PHP channels
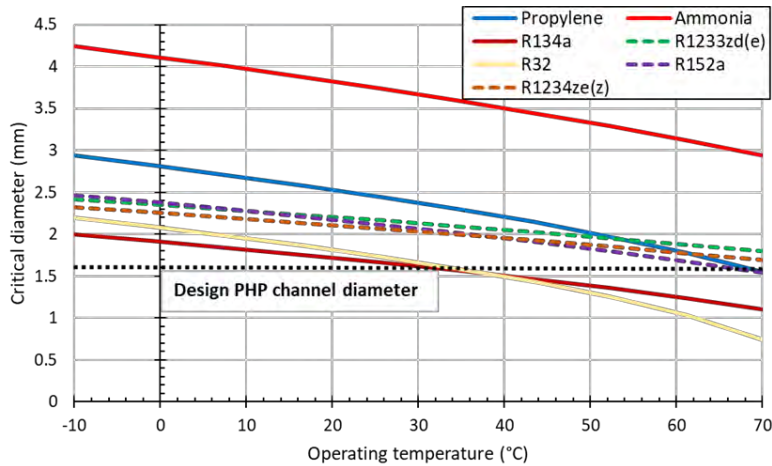

Figure 5. PHP channel critical diameter for various suitable working fluids

Figure 5 shows the critical channel diameter for various suitable PHP working fluids. While, alcohols can also be used, they are not considered because they exhibit low vapor pressure and require considerable start-up power for PHP to operate efficiently. Preliminary literature showed propylene and ammonia to have high performance merit number [12], which is calculated as:

$$M_{php} = \frac{\rho_l C_{pl}\left(\frac{\partial P}{\partial T}\right)_{sat} ZRT_{sat}}{h_{fg}\mu_l}$$

<div align="right">eq. 2</div>

Where, C_{pl} is the specific heat capacity in liquid state, Z is the compressibility factor, R is the gas constant, h_{fg} is the enthalpy of vaporization, and μ_l and the viscosity of the liquid.

Figure 6 shows the anticipated heat transfer limits of the PHP calculated according to equations presented in [7]. Propylene was considered as the working fluid in the analysis considering the relative ease and safety considerations compared to ammonia, and also the past experience in utilizing the working fluid in PHP performance testing [8,10]. In contrast to the HiK™ plate, the heat transfer limit of the PHP reduces with increasing operating temperature. The maximum heat transfer limit of the PHP is anticipated to be 340 W at 20 °C. The heat transfer limit reduces by a little over 50% to 165 W for an operating temperature of 40 °C. The maximum operating temperature is limited to ~ 67 °C and this is dictated by the Bond number limit for the channel diameter.
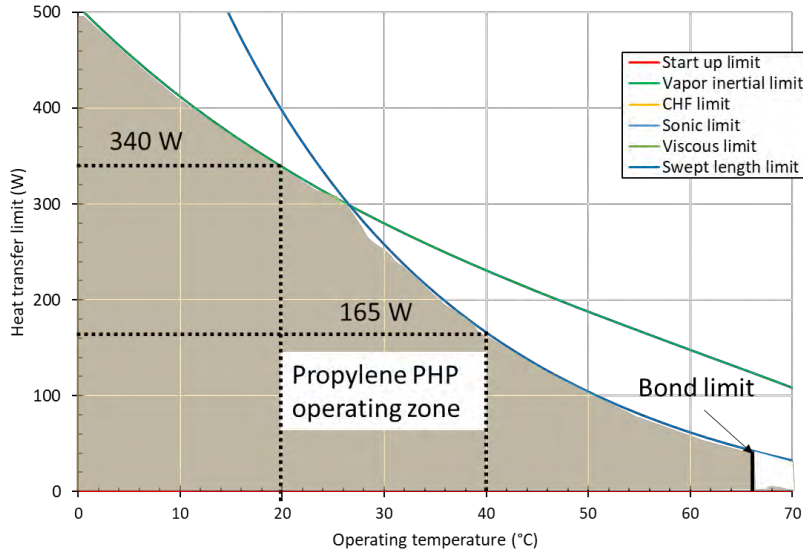
Figure 6. Anticipated heat transfer limits of the PHP

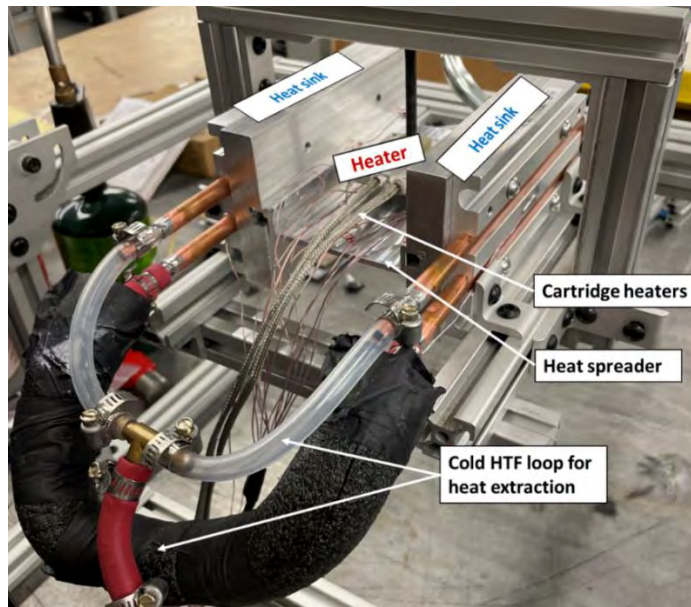## III.   Experimental System and Methodology

Figure 7. Heat spreader experimental system

A bench-top experimental system was assembled, as shown in Figure 7, for performance testing of the heat spreaders. A central heat source with two edge heat rejection through ICE-Lok® type configuration was considered for performance analysis. The heat source was a makeshift aluminum block of size 1-inch x 1-inch with two cartridge heater rod inserts. Two cold plates were mounted on a makeshift aluminum block. Together, they were used as the heat sink through ICE-Lok®. Propylene glycol was used as the cold HTF for heat extraction from the heat spreader. The HTF was circulated at a constant temperature by means of a constant temperature liquid bath (chiller).
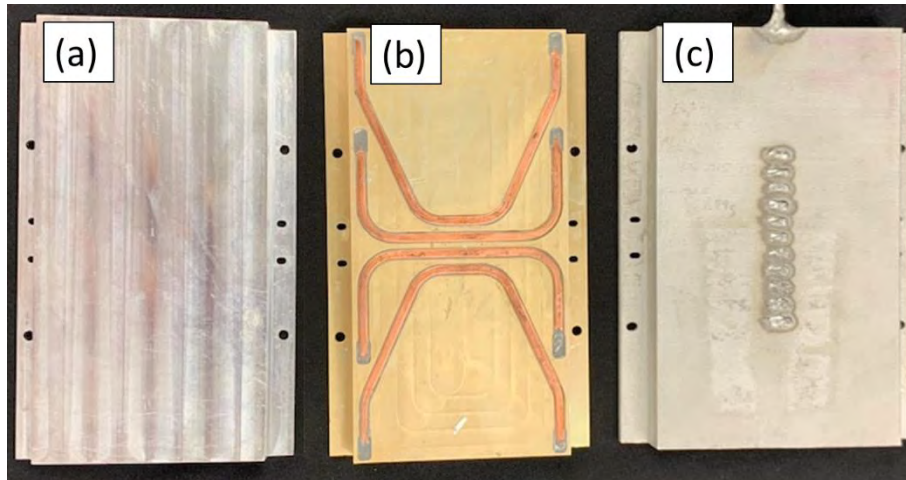
International Conference on Environmental Systems

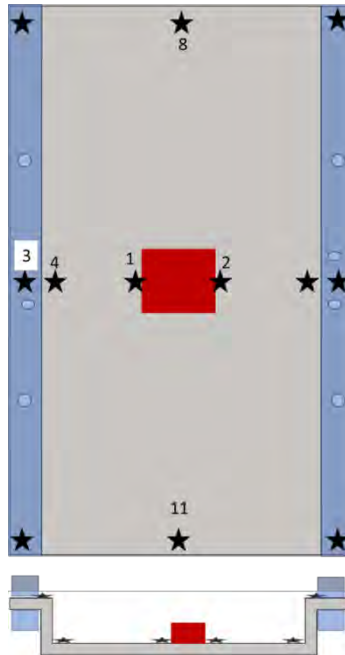**Figure 8. (a) conduction plate; (b) EHP; (c) PHP heat spreaders for performance testing**

Figure 9. Thermocouple layout and notation

Figure 8 shows the three heat spreaders, conduction plate heat spreader, EHP (HiK™ plate) heat spreader, and PHP heat spreaders. The heat spreaders were attached to the test system for performance testing. Quasi-steady state testing method was adopted with incremental heater powers to determine the performance of the heat spreaders. The thermocouple location and notation for performance testing is shown in Figure 9. TC1 represents the heat source (evaporator) temperature, while the thermocouple on edge of the plate (TC3) was the heat rejection (condenser) temperatures. TC8 and TC11 represented the plate lateral edge temperature due to heat spreading by the heat spreader. The heat spreader thermal performance was determined by calculating the thermal conductance as:

$$C = \frac{Q}{\Delta T}$$
eq. 3

Where, C is the thermal conductance of the heat spreader, Q is the thermal power, and ΔT is the average heat source (evaporator) and heat rejection (condenser) temperatures. Since the testing configuration represents two condensers with one evaporator, the thermal power for heat spreader performance calculation was half of applied heater power. The instrumentation error is summarized in Table 2.

7

Table 2. System instrument error for heat spreader performance testing

Instrument	Error
Thermocouple (°C)	±0.5 °C
Heater power (W)	±3 W

IV. Thermal Performance Testing of the Heat Spreaders

The thermal performance testing of the heat spreader was performed in a horizontal orientation at operating temperatures of 20 °C and 40 °C. The coolant was supplied at a constant temperature and so was used as the operating temperature. Firstly, the baseline performance of the conduction plate heat spreader was established. Then performance of the two-phase heat spreaders was determined and compared to each other. For brevity, the temperature profile of the heat spreader at 20 °C is shown for the heat spreaders. The testing was stopped when either dry-out occurred in the heat spreader or the maximum temperature on the heat spreader was 70 °C. The heat source temperature (TC1) on the heat spreader is represented in red color and the heat rejection temperature (TC3) on the stepped plane on the heat spreader is represented in the blue color. TC4 is the heat spreader edge temperature on the same plane (before the step turn) on the heat spreader. Fluid temperature is represented in dotted purple line and the heater power in dotted black line with values on the secondary right hand vertical axis.

A. Baseline thermal performance of conduction plate
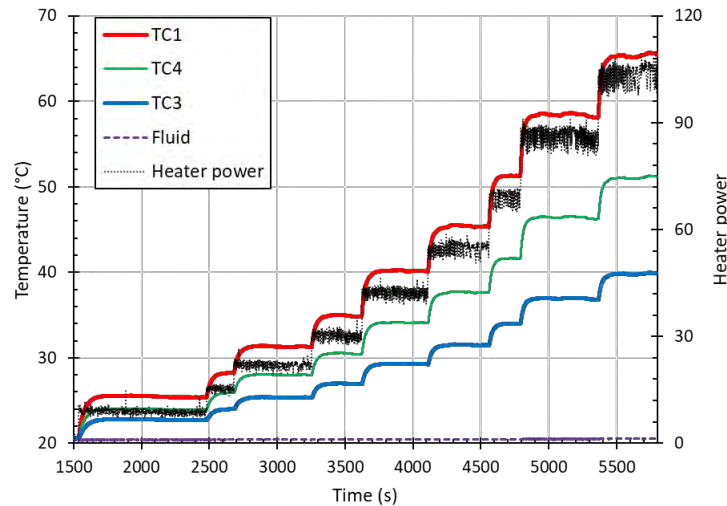

Figure 10. Wall temperature profile of conduction plate heat spreader

Thermal performance of the aluminum conduction plate heat spreader was first established as the baseline. Figure 10 shows the conduction plate heat spreader temperature profile with incremental heater power. The wall temperatures increase with the increasing heater power along with a proportional increase in ΔT between the heater source (TC1) and the heat rejection (TC4) temperatures. Maximum temperature of ~ 66.7 °C was recorded on the conduction plate heat spreader when the heater power was 105 W. The heat rejection temperature at TC3 was ~ 40 °C. After this point, the testing was stopped.

Figure 11 shows the thermal conductance of the conduction plate heat spreader at 20 °C and 40 °C operating temperatures. The average thermal conductance of the conduction plate heat spreader was 1.86±0.08 W/°C. Some variation in the thermal conductance was noticed which could be attributed to some instrument measurement error, and also some heat loss through the insulation. After system assembly, a 1-inch-thick insulation was applied on the heat spreader. Preliminary assessment for heat loss through the insulation calculated using equivalent heat transfer coefficient of 3 W/m^2-K [13] was 4.8 W. This parasitic heat loss through the insulation was 4.55% at heater power of 105 W.
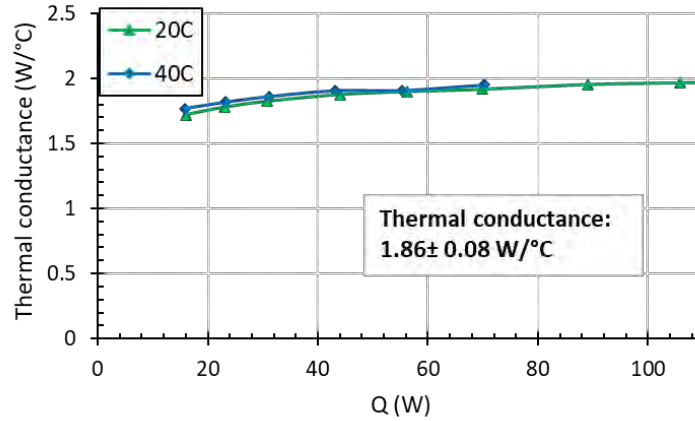
Figure 11. Thermal conductance of conduction plate heat spreader

B. Wall temperature profile of EHP (HiK™ plate) and PHP heat spreader at 20 °C and 40 °C
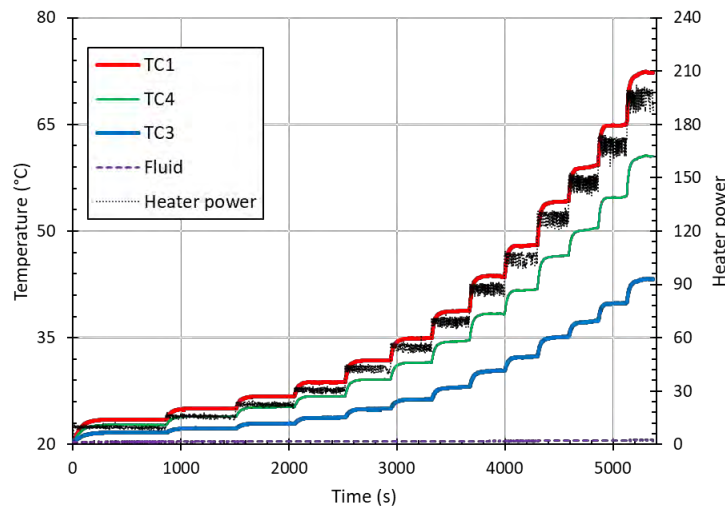

Figure 12. Wall temperature profile of EHP heat spreader at 20 °C operating temperature

Figure 12 shows the EHP heat spreader wall temperature at 20 °C operating temperature with incremental heater power. Maximum EHP temperature of ~ 72.5 °C was recorded when the heater power was 195 W. The ΔT between TC1 and TC3 was ~ 43.3 °C. However, it must be noted that the heat pipe condensers are on the same plane as the heat source, so temperature drop in the heat spreader due to the addition of the heat pipe was 12 °C between TC1 and TC4. Performance testing was stopped beyond this point. No dry-out was noticed in the EHP heat spreader.

Figure 13 shows the wall temperature profile of the PHP heat spreader 20 °C operating temperature with incremental heater power. Some pulsation in the wall temperatures was noticed, which is the characteristic of the PHP operation. The wall temperature profiles increased with increasing heater power. When the applied heater power was 88 W, the maximum (evaporator) PHP heat spreader temperature was 50.8 °C. However, when the heater power was incremented to 105 W, the evaporator wall temperature continued to increase. The condenser temperature increased temporally, but then reduced. This indicated a full dry-out of the PHP.
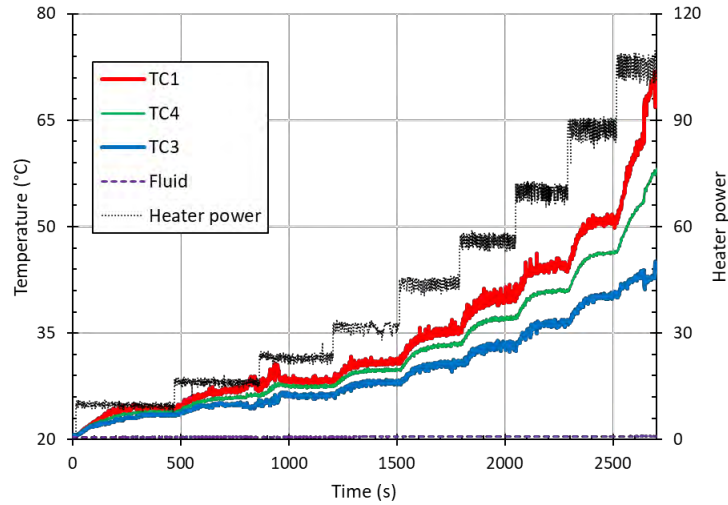
International Conference on Environmental Systems

Figure 13. Wall temperature profile of PHP heat spreader at 20 °C operating temperature

C. Wall temperature profile of EHP (HiK™ plate) and PHP heat spreader at 40 °C operating temperature
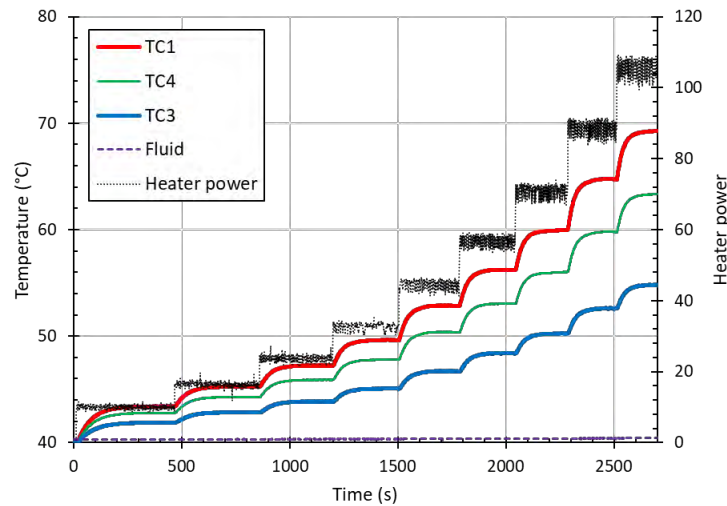

Figure 14. Wall temperature profile of EHP heat spreader at 40 °C operating temperature

Figure 14 shows the EHP wall temperature profile at 40 °C operating temperature. The temperatures increased with increasing heater powers. Maximum heat spreader temperature of 69.2 °C was recorded at a heater power of 105 W. The overall ΔT between TC1 and TC3 was 14.4 °C, while within the same plane with heat pipe condenser was only 6.5 °C. It was noted that the temperature drop between TC4 and TC3, which is due to heat transfer by material conduction was about 8.5 °C. Performance testing was stopped after this point.

Figure 15 shows the PHP heat spreader wall temperature at 40 °C operating temperature. No clear steady state operation was noted during the performance testing. Additionally, more vigorous pulsations in the PHP wall temperature was observed, especially with increasing heater power as the PHP temperature increased. The temporal changes in the temperature corresponded to simultaneous local temperature increase (decrease) in the evaporator (condenser) and vice-versa due to the liquid slug in the PHP channels especially in the heated length zone. Maximum temperature crossed 70 °C when the applied heater power was 45 W.
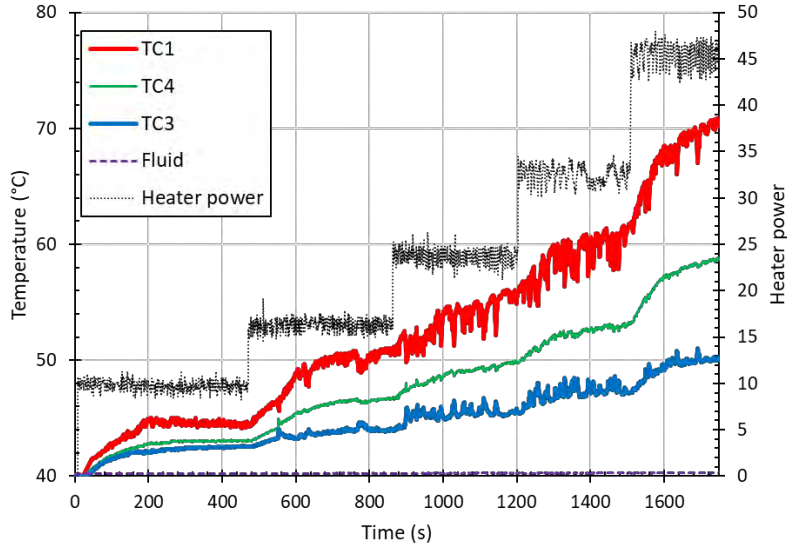
International Conference on Environmental Systems

Figure 15. Wall temperature profile of PHP heat spreader at 40 °C operating temperature

D. Performance comparison of EHP (HiK™ plate) and PHP heat spreaders
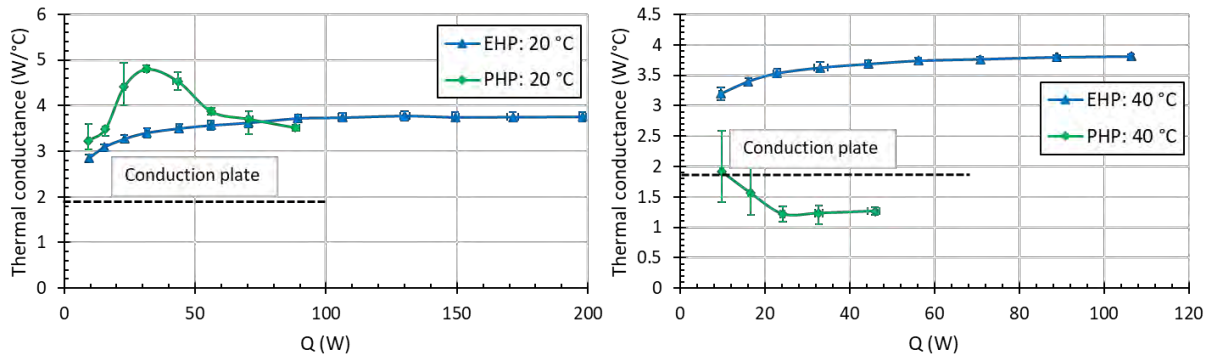

Figure 16. Thermal conductance of EHP and PHP heat spreaders

Figure 16 shows the thermal conductance of the EHP and the PHP heat spreaders. For reference, the thermal conductance of the conduction plate is given as dotted black lines. At operating temperature of 20 °C, the thermal conductance of the PHP was slightly better than the EHP at lower heater powers. In the case of the PHP, the error margin is slightly higher and is easily susceptible to variations in overall ΔT between the evaporator and the condenser temperatures, especially at lower heater powers. For example, when the heater power is 23 W, ΔT of 2.3 °C corresponds to thermal conductance of ~ 5 W/°C, while a ΔT of 2.8 °C will yield a thermal conductance of ~ 4.1 W/°C. As the heater power increases above 50 W, it can be noted that the PHP potentially operates in a partial dry-out condition, and this can be evidenced by increasing amplitude of pulsation in the wall temperatures. As heater power increases, the dry-out portion in the PHP increases, eventually, occurs when the heater power increased from 88 W to 105 W. The thermal conductance of the EHP, on the other hand, increased from slightly below 3 W/°C to 3.7-3.8 W/°C, which is about 100% higher than the conduction plate. No, dry-out in the EHP was observed. At 40 °C operating temperature, the PHP operated at partial dry-out phenomenon even at lower heater powers. On the other hand, the thermal conductance of the EHP was about 3.8 W/°C, indicating EHP to be more suitable heat spreader at this operating condition.

International Conference on Environmental Systems

V. Near Term Plans for Performance Testing of the Heat Spreaders

In the near term, more comprehensive performance testing of the heat spreaders will be performed and the updated results will be presented at the conference. Firstly, the test matrix will redefine the operating temperature from the coolant to the heat spreader condenser temperature. During performance testing, it was noted that the chiller had a limited heat rejection capacity to match the higher heater power loads. So, structural changes to regulate and adapt the coolant temperature will be implemented to keep the heat spreader condenser at a constant temperature by employing auxiliary booster heat exchangers to facilitate heat rejection by liquid nitrogen. Comprehensive performance testing will be performed by incorporating these above changes and presented for following design parameters of interest:

- Heat spreading in the lateral direction will be discussed by analyzing temperature drop from TC1 to TC8/TC11 in the heat spreaders.
- EHP: The EHP tested consists of 2 Cu screen wraps. Another EHP with 3 Cu screen wraps will be fabricated and tested. Additional screen wrap will allow for further improvement in heat transfer limit with a meager compromise in the thermal performance.
- PHP: Currently, testing is performed with propylene as the working fluid. Testing will be extended to include alternate working fluids like ammonia, R1233zd(e) etc.
- Influence of gravity: In the test results showed here, the heat spreaders were tested in the horizontal configuration. In future tests, the influence of gravity on the heat spreader performance will be determined.

VI. Conclusions

Two phase heat spreaders based on the embedded heat pipe (EHP) and the pulsating heat pipe (PHP) were fabricated and the performance was compared. EHP consisted of 4 copper-water heat pipes in a U-shape layout. The Propylene was used as the working fluid in the PHP. Testing was performed in a central heating-two edge heat rejection configuration. The thermal conductance of the baseline aluminum conduction plate was 1.86±0.08 W/°C. At coolant temperature of 20 °C, the thermal conductance of the PHP was slightly better than the EHP at lower heater powers, < 50 W. As heater power increased, PHP operated in a partial dry-out mode eventually drying out at a heater power of 105 W. The thermal conductance of the EHP was about 100% more than the conduction plate. At a higher operating temperature of 40 °C, the PHP operated at a dry-out condition with a significantly lower thermal conductance, while, the EHP operated normally. In near term, strategic changes will be made in the testing method and updated results will be presented at the conference.

Acknowledgments

References

[1] R. Oeftering, J.F. Soeder, and Ray Beach. Analysis of Advanced Modular Power Systems (AMPS) for Deep Space Exploration, Space Power Workshop. No. GRC-E-DAA-TN14436. 2014.

[2] SPACE VPX™ - Next Generation Space Interconnect Standard (NGSIS) Space VPX and SpaceVPX Lite Tutorial

[3] S. M. S. Murshed and C. A. N. de Castro, A critical review of traditional and emerging techniques and fluids for electronics cooling, Renewable and Sustainable Energy Reviews, vol. 78, pp. 821-833, 2017.

[4] https://www.1-act.com/products/hik-plates/

[5] https://www.1-act.com/when-to-use-heat-pipes-hik-plates-vapor-chambers-and-conduction-cooling/hik-plates/?hilite=Hi-K+plate

[6] M. Mameli, M. Marengo and S. Zinna, Numerical model of a multi-turn Closed Loop Pulsating Heat Pipe: Effects of the local pressure losses due to meanderings, International Journal of Heat and Mass Transfer, vol. 55, pp. 1036-1047, 2012.

[7] B. Drolen and C. Smoot, Performance limits of oscillating heat pipes: Theory and validation, Journal of Thermophysics and Heat Transfer, vol. 31, no. 4, pp. 920-936, 2017

[8] K.L. Lee, S.K. Hota, A. Lutz, S. Rokkam, Advanced Two-Phase Cooling System for Modular Power Electronics, 51st International Conference on Environmental Systems (ICES), St. Paul, Mn, 2022

[9] ANSI/VITA 48.2-2020, "Mechanical Standard for VPX REDI Conduction Cooling," VITA, 2020

[10] S.K. Hota, K.L. Lee, G. Hoeschele, R. Bonner, S. Rokkam, Experimental Comparison on Thermal Performance of Pulsating Heat Pipe and Embedded Heat Pipe Heat Spreaders, 2023 39th Annual Semiconductor Thermal Measurement, Modeling and Management Symposium (SEMI-THERM), 2023.

[11] https://www.1-act.com/products/ice-lok-thermally-enhanced-wedgelock/

[12] J. Kim and S. J. Kim, Experimental investigation on working fluid selection in a micro pulsating heat pipe, Energy Conversion and Management, vol. 205, p. 112462, 2020

[13] T.L. Bergman, F.P. Incropera, D.P. Dewitt, A.S. Lavine, Fundamentals of Heat and Mass Transfer, John Wiley & Sons, 2011.

International Conference on Environmental Systems